

PAPER • OPEN ACCESS

Mechanical impact of dynamic phenomena in Francis turbines at off design conditions

To cite this article: F Duparchy *et al* 2017 *J. Phys.: Conf. Ser.* **813** 012035

View the [article online](#) for updates and enhancements.

Related content

- [Study on the effect of the runner design parameters on 50 MW Francis hydro turbine model performance](#)
Ujjwal Shrestha, Zhenmu Chen and Young-Do Choi
- [Performance Comparison of Optimized Designs of Francis Turbines Exposed to Sediment Erosion in various Operating Conditions](#)
K P Shrestha, S Chitrakar, B Thapa et al.
- [Francis-99 Workshop 2: transient operation of Francis turbines](#)

Recent citations

- [Swirl number based transposition of flow-induced mechanical stresses from reduced scale to full-size Francis turbine runners](#)
A. Favrel *et al*
- [Operating conditions leading to crack propagation in turbine blades of tidal barrages. Influence of head and operating mode](#)
Yongyao Luo *et al*



IOP | ebooks™

Bringing together innovative digital publishing with leading authors from the global scientific community.

Start exploring the collection—download the first chapter of every title for free.

Mechanical impact of dynamic phenomena in Francis turbines at off design conditions

F Duparchy¹, J Brammer¹, M Thibaud¹, A Favrel², P Y Lowys¹, F Avellan²

¹GE Renewable Energy, Hydro Solutions, 82 Avenue Léon Blum – BP75, 38041 Grenoble Cedex 9, France

²EPFL Laboratory for Hydraulic Machines, Avenue de Cour 33 bis, 1007 Lausanne, Switzerland

E-mail: florian.duparchy@ge.com

Abstract. At partial load and overload conditions, Francis turbines are subjected to hydraulic instabilities that can potentially result in high dynamic solicitations of the turbine components and significantly reduce their lifetime. This study presents both experimental data and numerical simulations that were used as complementary approaches to study these dynamic solicitations. Measurements performed on a reduced scale physical model, including a special runner instrumented with on-board strain gauges and pressure sensors, were used to investigate the dynamic phenomena experienced by the runner. They were also taken as reference to validate the numerical simulation results. After validation, advantage was taken from the numerical simulations to highlight the mechanical response of the structure to the unsteady hydraulic phenomena, as well as their impact on the fatigue damage of the runner.

1. Introduction

The increasing need of flexibility for single regulated hydro turbines, such as Francis units, tends to increase the number of hours in operation at partial load and overload conditions, outside of the best operating range for which the turbines were originally designed. In these off-design conditions, hydraulic instabilities can occur. They are the source of high dynamic solicitations that can potentially reduce the lifetime of the components of the turbine, and especially the runner.

Today, numerical simulations can help to understand the dynamic loading applied on the structure as well as its mechanical response. However, modelling accurately such complex phenomena remains challenging. In some cases, it is necessary to further validate the results of the simulations with experimental data, from both a hydraulic and mechanical point of view. In this study, an experimental investigation was performed on a reduced scale physical model of a Francis turbine including an instrumented runner equipped with on-board strain gauges and pressure sensors. In parallel, Computational Fluid Dynamics (CFD) and Finite Element Analysis (FEA) simulations were performed for three operating points corresponding to deep partial load, partial load and overload conditions. The results were then compared with the experimental data. Once consistency between them was achieved, advantage was taken from the numerical simulations to highlight the differences in terms of mechanical behaviour of the runner when subjected to the identified hydraulic phenomena.



2. Experimental setup

The test case consisted of a reduced scale physical model of a Francis turbine with 16 blades and 20 guide vanes. It was installed on the test rig PF3 of the Laboratory for Hydraulic Machines (EPFL-LMH) operating in closed loop. The tests were performed in cavitation conditions corresponding to the full-scale turbine conditions.

The instrumentation included a set of pressure sensors distributed along the reduced scale model. In particular, pressure fluctuations were measured in the draft tube cone, where two sections were equipped with 4 flush-mounted pressure sensors (figure 1).

In addition to this standard set of sensors, an instrumented runner was used. It was instrumented with pressure sensors and strain gauges (figure 1). It was specifically designed to measure both the hydraulic pressure fluctuations applied on the blades as well as the mechanical response of the structure. The signals were transmitted to the stationary parts through a telemetry system.

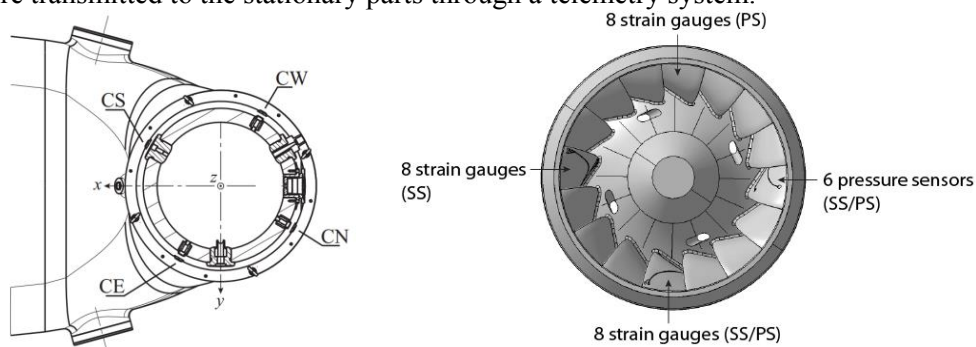


Figure 1: Cut view of the upper section of the draft tube cone with the pressure sensors (left) and instrumented runner with the location and number of the strain gauges (SS: suction side, PS: pressure side) (right)

3. Selection of the calculated points

To identify the relevant operating points to use in the numerical simulations, the experimental data was first analysed. For a fixed n_{ED} value, corresponding to the nominal n_{ED} value, the evolution of the dynamic blade strain over the discharge can be divided into different zones, as shown in Figure 2. n_{ED} and Q_{ED} coefficients are defined according to IEC standard 60193:1999.

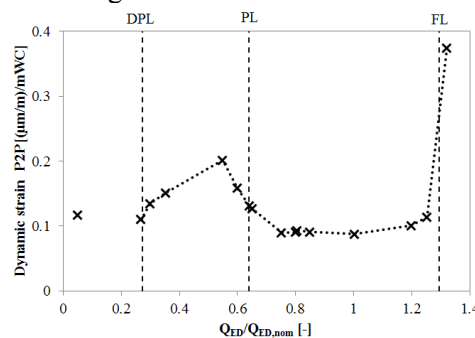


Figure 2: Dynamic strain measurement on a load variation for a strain gauge located close to the trailing edge of the pressure side of the blade, close to the hub.

Around the nominal Q_{ED} value ($0.8 < Q_{ED}/Q_{ED,nom} < 1.2$), the dynamic strain was low. For this zone, only the rotor-stator interaction (RSI) was identified in the frequency spectra, at $20 \cdot f_0$, where f_0 is the rotational frequency of the runner.

At full load ($Q_{ED}/Q_{ED,nom} > 1.2$), a significant increase of dynamic strain was observed. It was caused by a self-excited pressure surge due to the presence of the full load axial vortex rope [1]. Its fundamental frequency was $0.23 \cdot f_0$ and several harmonics were observed (figure 3c).

At partial load ($0.3 < Q_{ED}/Q_{ED,nom} < 0.8$), a second dynamic strain elevation was identified. It corresponded to the part load helical vortex zone, with a typical frequency of $0.70 \cdot f_0$ in the rotating frame of the runner [3] (figure 3b). This frequency reached its maximum intensity at around $Q_{ED}/Q_{ED,nom} = 0.55$ [2].

At deep partial load, ($Q_{ED}/Q_{ED,nom} < 0.3$), a global elevation of the spectrum was observed, without clear emergence, except for the RSI (figure 3a). It means that the loading is of a stochastic nature. However, the peak-to-peak dynamic strain was low. It should be noted that for this operating point no inter blade cavitation vortex was observed.

Finally, three operating points were selected for the numerical study (figure 2): at full load $Q_{ED}/Q_{ED,nom} = 1.30$ (FL), partial load $Q_{ED}/Q_{ED,nom} = 0.64$ (PL) and deep partial load $Q_{ED}/Q_{ED,nom} = 0.27$ (DPL).

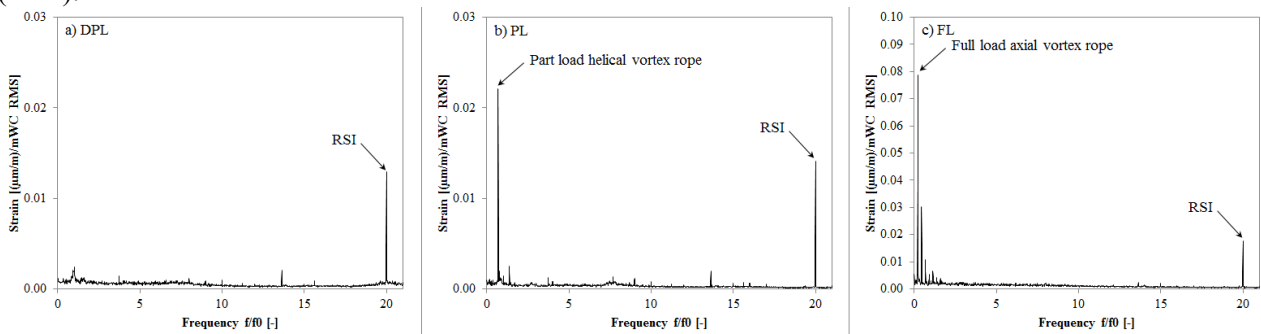


Figure 3: Frequency spectra for the three operating points selected for the numerical study. Different scale for FL.

For the selected operating points, CFD and FEA simulations were performed with ANSYS software. The unsteady CFD simulations generated pressure fields that were then used as an input for the FEA study.

4. Numerical modelling

4.1. CFD simulation

Each selected operating point exhibited different hydraulic and mechanical characteristics, and therefore the complexity of each CFD model was adapted to calculate them as accurately as possible. Each Hyperbole project partner was allocated an operating point, and such differences include the mesh refinement, the turbulence model and the time step. Also, for the full load calculation it was necessary to impose a fluctuating pressure level at the spiral case inlet to simplify and represent the hydro-acoustic characteristics. These unsteady calculations had the additional complexity of modelling cavitation, so the choice of cavitation model was also considered, and sensitivity tests were performed to confirm the results.

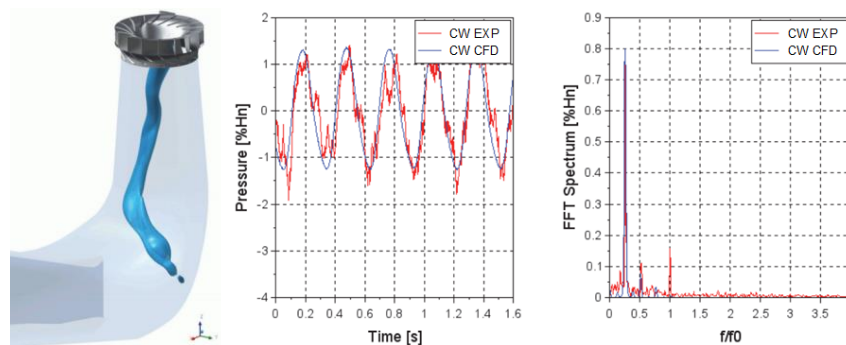


Figure 4: Part load operation: CFD flow visualisation (left) and draft tube pressure fluctuation comparisons between CFD and experimentation (right)

Before using the CFD pressure fields to perform FEA simulations it was crucial to have confidence in the CFD results, otherwise any errors would be passed on to the mechanical analysis. For this purpose, CFD simulations were validated by comparison with the experimental results. Figure 4 shows such an example for the part load vortex rope. As well as confirming visually that the cavitating vortex rope in the CFD corresponded to what was observed on the test rig, pressure sensor measurements were also

compared and FFT analysis showed that both frequency and amplitude of the part load vortex rope were well predicted.

4.2. FEA simulation

For the mechanical simulation, the entire runner was considered, including the blade cavities made for the strain gauges and the grooves for the wires. The mesh was refined around the strain gauge locations and a set of two nodes was used to extract the strain values at the exact position and direction of the gauges. This enabled an accurate comparison of the results of the simulation with the measurement. A total of 2.3M nodes were used (figure 5).

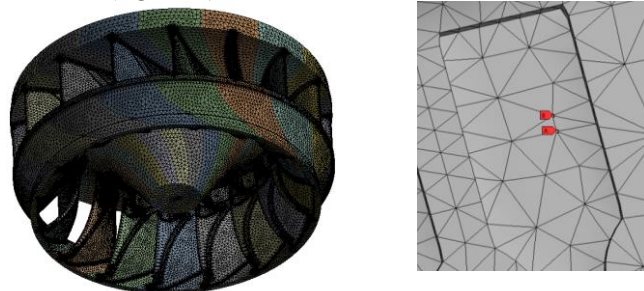


Figure 5: FEA model and meshing (left) and detail of the strain gauge imprint mesh (right)

Considering that the natural frequencies of the runner were much higher than the excitation frequencies contained in the CFD pressure fields, a quasi-static approach was used, i.e. successive static calculations were performed. The hydraulic load was applied in several time steps in order to capture the maximum stress variation. The time step was selected to be consistent with the frequencies of the cavitation phenomena observed in off-design conditions.

Results of FEA analysis were compared to the experimental data. First, the time signals were superimposed to qualitatively check that they had a similar evolution (figure 6). At this stage, it was observed that the time step was sufficient to simulate low frequency phenomena such as the vortex rope, while high frequency solicitations such as RSI were roughly described. It was also checked that RSI could also be modelled accurately by repeating the simulation at DPL with a refined angular step.

Finally, the peak-to-peak strain values were compared with the measurements (figure 6) and they showed a good agreement with the experimental results, except for some strain gauges for which measurement issues were suspected.

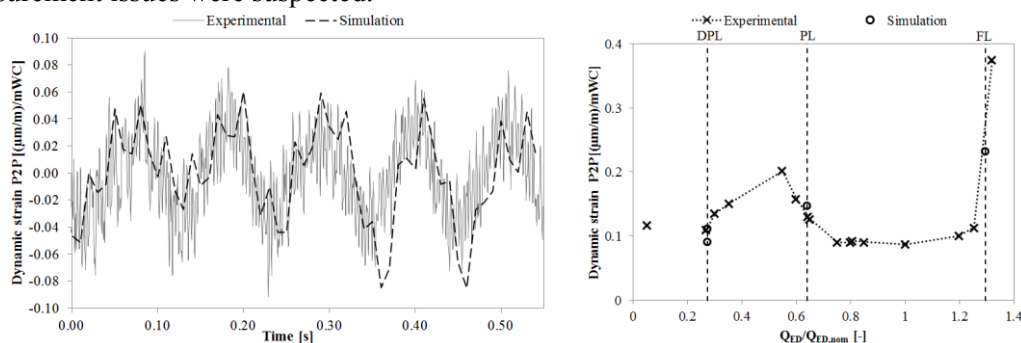


Figure 6: Comparison between simulations and measurements. Time signal of a strain gauge at PL (left) and comparison of peak-to-peak values for the three calculated points (right)

5. Impact on fatigue damage

The good correlation between simulation and measurement gave confidence to the fact that the physics of the phenomena, as well as the reaction of the structure, was well predicted. The simulations were used to understand how the structure behaved in the presence of the different hydraulic phenomena. Contrary to the measurements that gave information only for a limited number of sensor locations, the numerical simulations provided results at each node of the model. Numerical results were therefore used

to highlight the differences of behaviour for each operating point, in terms of structure displacement, stress distribution and stress concentration, as shown in Figure 7.

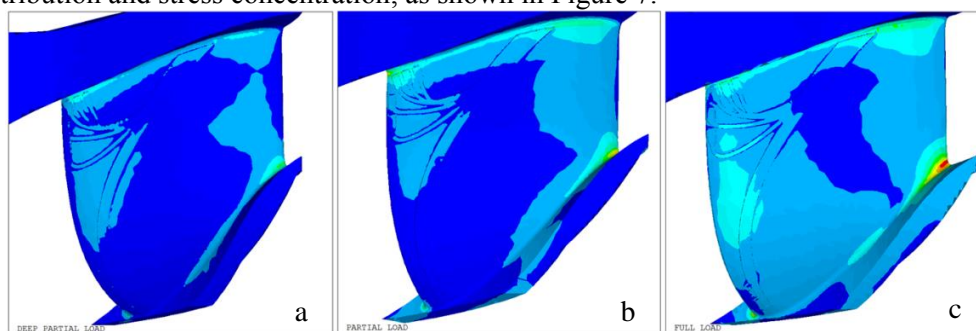


Figure 7: Dynamic stress distribution for deep part load (a), part load (b) and full load (c). Same scale (red color corresponds to highest stress)

Moreover, hot spot factors that link the dynamic strain at the strain gauge locations to the maximum stressed area of the runner were extracted from the simulation and used to extrapolate the measurement. A Rainflow cycle counting algorithm was then applied to the extrapolated signals and fatigue damage was compared for each operating point (Figure 8).

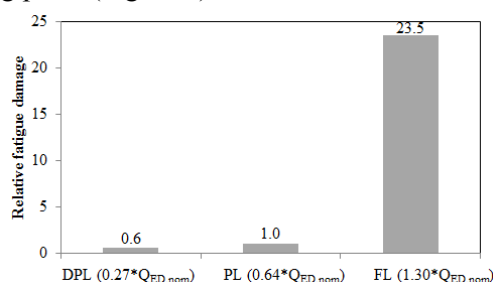


Figure 8: Relative fatigue damage calculated at the trailing edge of the blade-to-hub junction

6. Conclusion

Coupled unsteady CFD and FEA simulations showed good capability to capture hydraulic phenomena that occur at off-design conditions and their mechanical impact on the runner. The results were validated by comparison with measurements performed on a reduced scale physical model that included a special runner equipped with on-board sensors.

These two complementary approaches were used to investigate the impact of each dynamic phenomenon on the mechanical behaviour and the fatigue damage of the runner. This method can be used not only for existing designs but also for new projects [4].

An additional measurement campaign on the full scale industrial turbine, including runner strain gauges and pressure sensors has also been carried out. Therefore, the transposition of the dynamic solicitations from the reduced scale model to full-scale runner will be studied.

Acknowledgments

The research leading to the results published in this paper is part of the HYPERBOLE research project, granted by the European Commission (ERC/FP7- ENERGY-2013-1-Grant 608532).

References

- [1] Müller A, Dreyer M, Andreini N and Avellan F 2013 *Experiments in Fluids* **54**(4):1-11
- [2] Favrel A, Müller A, Landry C, Yamamoto K and Avellan F 2015 *Experiments in Fluids* **56**:215
- [3] Duparchy F, Favrel A, Lowys P Y, Landry C, Müller A, Yamamoto K and Avellan F 2016 *Journal of Physics: Conference Series* **656** 012061 (CAV2015, Lausanne, Switzerland)
- [4] Brammer J, Duparchy F, Lowys P Y, Thibaud M, Wheeler K and De Colombel T 2016 *Increasing the operating range of Francis turbine by considering dynamic phenomena at partial load*, Hydro 2016, Montreux, Switzerland